J. Org. Chem. **1995,** *60,* 1033−1038 **1033**

Synthesis and Electrochemical Properties of Redox-Active [2]Rotaxanes Based on the Inclusion Complexation of 1,4-Phenylenediamine and Benzidine by Cyclobis(paraquat-*p*-phenylene)

Emilio Córdova, Richard A. Bissell, and Angel E. Kaifer*

Chemistry Department, University of Miami, Coral Gables, Florida 33124

Received November 22, 1994⊗

The inclusion complexation of 1,4-phenylenediamine (**2**) by the host cyclobis(paraquat-*p*-phenylene) (**1**$^{4+}$) was used as the core interaction for the template-directed synthesis of a new redox-active [2]rotaxane (**5**$^{4+}$) in high yield. The half-wave potentials for both monoelectronic oxidations of the 1,4-phenylenediamine subunit in this rotaxane exhibit remarkable anodic shifts as compared to the values typically observed in 1,4-phenylenediamine derivatives. These shifts result from the hindrance imposed by the rotaxane's tetracationic macrocyclic bead on the generation of additional positive charges. The electrostatic field created by the bead also slows down the kinetics of electron transfer, especially for the second oxidation process. Qualitatively similar effects were observed on the electrochemistry of a comparable rotaxane (**7**$^{4+}$) built around the interactions between a benzidine subunit and host **1**$^{4+}$, but the magnitude of the effects on the voltammetric parameters was smaller than in **5**$^{4+}$.

Introduction

In the last six years Stoddart and co-workers have used the electron-deficient receptor **1**$^{4+}$ as a key component for the self-assembly of a series of fascinating rotaxane and catenane structures.[1] We have recently reported[2] the self-assembly of rotaxanes based on the noncovalent interactions between **1**$^{4+}$ and several biphenyl guests and applied these interactions to the preparation of a *chemically and electrochemically controllable molecular shuttle.*[3] A molecular shuttle[4] is a type of rotaxane which contains two "stations" along the thread of the dumbbell component and only one bead. Typically, these stations are aromatic subunits that provide some stabilization to the bead, which therefore shuttles back and forth between them. In Stoddart's design,[5] the molecular shuttle's active components are two π-donor stations in the thread of the dumbbell component and one π-acceptor bead. The optimization and control of bead dynamics in these systems require detailed investigations of the interactions between the receptor and a variety of π-donor guests, as well as the development of methods to modulate the strength of the station−bead interactions. As part of these studies, we report here the synthesis and properties of a novel rotaxane based on the inclusion complexation of 1,4-phenylenediamine (**2**) by host **1**$^{4+}$. Guest **2** is structurally very similar to 1,4-hydroquinol, which was the foundation of earlier work.[1,4,5] However, both guests differ considerably in their redox-behavior, since 1,4-phenylenediamine is substantially more susceptible to oxidation than 1,4-hydroquinol. In this work, we compare the electrochemical behavior of rotaxanes containing either 1,4-phenylenediamine or benzidine (**3**) as the π-donor stations in the thread of the dumbbell components.

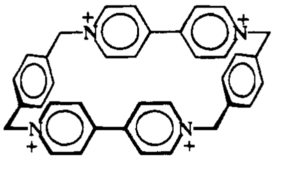

1^{4+}

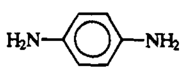

2

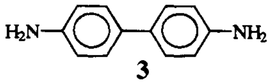

3

Experimental Section

Materials. Benzidine (Fluka), 1,4-phenylenediamine (Aldrich), and tetrabutylammonium hexafluorophosphate (Fluka, puriss) were used as received. The cyclophane receptor **1**$^{4+}$ was synthesized and isolated as its tetrakis(hexafluorophosphate) salt according to the reported procedure.[1] Acetonitrile (Aldrich, 99.9+%, HPLC grade) was dried by reflux over CaH_2 and distilled under a nitrogen atmosphere immediately prior to use. All other chemicals were of the best commercial quality available.

***N,N'*-Bis[((hydroxyethoxy)ethoxy)ethyl]-*p*-phenylenediamine (4).** A solution containing *p*-phenylenediamine (5 g, 46.2 mmol) in dry CH_3CN (50 mL) was added to a suspension of K_2CO_3 (15.2 g, 110 mmol) in dry CH_3CN (60 mL) over 30 min. A solution of 2-[2-(2-chloroethoxy)ethoxy]ethanol (17 g, 100 mmol) in CH_3CN (20 mL) was added to the stirred solution. The solution was then heated to reflux under nitrogen for 3 days. The reaction mixture was cooled down and filtered, and the filtrate was evaporated in vacuo. The product was purified by column chromatography (SiO_2, 50:50 ethyl acetate−acetone) to yield a reddish oil (4.3 g, 25%). The product was stored under nitrogen and kept protected from light. ^1H NMR (400 MHz, $CDCl_3$) δ 3.24 (4H, t), 3.69 (20H, m), 6.15 (4H, s). HRMS: Calcd for $C_{18}H_{32}N_2O_6$: *m/e* 372.226037. Found: *m/e* 372.22530. Anal. Calcd for $C_{18}H_{34}N_2O_6{\cdot}H_2O$: C, 55.37; H, 8.78; N, 7.17. Found: C, 55.92; H, 8.48; N, 7.25.

Phenylenediamine Rotaxane (5^{4+}). Cyclobis(paraquat-*p*-phenylene) **1**$^{4+}$ (67 mg, 0.06 mmol), **4** (67 mg, 0.18 mmol),

---

⊗ Abstract published in *Advance ACS Abstracts,* February 1, 1995.

[1] Anelli, P. L.; Ashton, P. R.; Ballarini, R.; Balzani, V.; Delgado, M.; Gandolfi, M. T.; Goodnow, T. T.; Kaifer, A. E.; Philp, D.; Pietraszkiewicz, M.; Prodi, L.; Reddington, M. V.; Slawin, A. M. Z.; Spencer, N.; Stoddart, J. F.; Vicent, C.; Williams, D. J. *J. Am. Chem. Soc.* **1992,** *114,* 193.

[2] Córdova, E.; Bissell, R. A.; Spencer, N.; Ashton, P. R.; Stoddart, J. F.; Kaifer, A. E. *J. Org. Chem.* **1993,** *58,* 6550.

[3] Bissell, R. A.; Córdova, E.; Kaifer, A. E.; Stoddart, J. F. *Nature* **1994,** *369,* 133.

[4] Anelli, P. L.; Spencer, N.; Stoddart, J. F. *J. Am. Chem. Soc.* **1991,** *113,* 5131.

[5] (a) Stoddart, J. F. *Chem. Aust.* **1992,** *59,* 576. (b) Ashton, P. R.; Bissell, R. A.; Spencer, N. A.; Stoddart, J. F.; Tolley, M. S. *Synlett* **1992,** 914.

0022-3263/95/1960-1033$09.00/0

and 2,6-lutidine (0.049 mL, 0.42 mmol) were added to dry CH_3CN (2 mL). Triisopropylsilyl triflate (0.113 mL, 0.42 mmol) was added to the solution with stirring. The solution was stirred at room temperature for 2 days, after which the solvent was removed in vacuo. The residue was suspended in $CH_2Cl_2-Et_2O$, transferred to a tube, and centrifuged. After decantation of the solvent, the procedure was repeated three times. The residue was dissolved in $MeNO_2$ (5 mL) before adding CH_2Cl_2 (10 mL) to precipitate a white solid, which was separated by centrifugation, suspended in $CH_2Cl_2-MeNO_2$ (2:1, v/v, 6 mL), and centrifuged again. The combined organic solutions were evaporated in vacuo. The solid was purified by column chromatography [SiO_2, $MeOH-MeNO_2-$saturated NH_4PF_6 (165:35:5)] yielding a turquoise blue solid (46 mg, 43%). ^1H NMR (400 MHz, CD_3CN) δ 1.02 (42 H, m), 2.67 (4H, t), 3.11 (4H, s), 3.705 (4H, t), 3.75 (4H, t), 3.84 (4H, t), 3.91 (12H, m), 5.74 (8H, s), 7.86 (8H, s), 7.94 (8H, d), 8.90 (8H, d). FABMS (3-nitrobenzyl alcohol): 1640 $(M - PF_6)^+$, 1494 $(M - 2PF_6)^+$, 1349 $(M - 3PF_6)^+$, 1202 $(M - 4PF_6)^+$. Anal. Calcd for $C_{72}H_{104}N_6O_6Si_2P_4F_{24}$: C, 48.43; H, 5.87; N, 4.71. Found: C, 48.25; H, 5.92; N, 4.68.

***N,N'*-Bis[((hydroxyethoxy)ethoxy)ethyl]-4,4'-diaminobiphenyl (6).** A solution of 2-[2-(2-chloroethoxy)ethoxy]ethanol (20.2 g, 136.1 mmol) in benzene (40 mL) was added dropwise to a warm solution of benzidine (7 g, 45.5 mmol) and triethylamine (11.2 g, 112 mmol) in benzene (100 mL). The reaction mixture was refluxed under nitrogen for 2 weeks. The resulting solution was evaporated in vacuo, and the residue was taken up in chloroform (200 mL). The organic solution was washed with H_2O (3×50 mL) and dried ($MgSO_4$). The organic extract was evaporated in vacuo and purified by column chromatography [SiO_2, $CHCl_3-$acetone (2:1)], and the product was recrystallized from $EtOH/Et_2O$ to yield yellow bladelike crystals (7.54 g, 45%). ^1H NMR (400 MHz, CD_3CN) δ 2.73 (2H, t) 3.25–3.27 (4H, m), 3.50 (4H, t), 3.55–3.59 (12H, m), 3.64 (4H, t), 4.45 (2H, b), 6.66 (4H, d), 7.33 (4H, d). FABMS (3-nitrobenzyl alcohol): 448 (M^+). Anal. Calcd for $C_{24}H_{36}O_6N_2$: C, 64.26; H, 8.09; N, 6.25. Found: C, 64.15; H, 8.11; N, 6.32.

Benzidine Rotaxane (7^{4+}). Cyclobis(paraquat-*p*-phenylene) (67 mg, 0.06 mmol), **6** (82 mg, 0.18 mmol), and 2,6-lutidine (0.4 mL, 3.4 mmol) were added to dry DMF (3 mL). Triisopropylsilyl triflate (0.4 mL, 1.5 mmol) was added to the solution with stirring. The solution was stirred at room temperature for 2 days, after which the solvent was removed in vacuo. The residue was suspended in $CH_2Cl_2-Et_2O$, transferred to a tube, and centrifuged. After decantation of the solvent, this procedure was repeated three times. The residue was dissolved in $MeNO_2$ (5 mL) before adding CH_2Cl_2 (10 mL) to precipitate a white solid, which was separated by centrifugation, suspended in $CH_2Cl_2-MeNO_2$ (2:1 v/v, 6 mL), and centrifuged again. The combined organic solutions were evaporated in vacuo. The residue was then suspended in a solution of ethyl acetate$-Et_2O$ (10 mL) and filtered. The solid was purified by column chromatography [SiO_2, $MeOH-MeNO_2-$saturated NH_4PF_6 (165:35:5)] yielding a green solid (43 mg, 39%). ^1H NMR (400 MHz, CD_3CN) δ 1.05–1.09 (42H, m), 3.09 (4H, m), 3.61 (4H, t), 3.77–3.79 (12H, m), 3.83 (4H, t), 4.30 (2H, t), 4.76 (4H, d), 5.31 (4H, d), 5.76 (8H, s), 7.60 (8H, d), 7.90 (8H, s), 8.82 (8H, d). FABMS (3-nitrobenzyl alcohol): 1716 $(M - PF_6)^+$, 1571 $(M - 2PF_6)^+$, 1426 $(M - 3PF_6)^+$. Anal. Calcd for $C_{78}H_{108}O_6N_6Si_2P_4F_{24}\cdot 2H_2O$: C, 49.37; H, 5.95; H, 4.43. Found: C, 49.43; H, 5.85; N, 4.12.

Equipment. The electrochemical equipment has been described elsewhere.[6] Electronic absorption spectra were recorded with a Hewlett Packard 8452A or a Shimadzu UV-2102PC spectrophotometer. ^1H NMR spectra were recorded using a Varian VXR-400-S spectrometer. Mass spectra were obtained at the Mass Spectroscopy Facility of the University of Illinois at Urbana–Champaign. FAB mass spectra of the two rotaxane samples were recorded at the University of Birmingham. Combustion analyses were performed by Atlantic Microlab in Norcross, GA.

Determination of Binding Constants. The complexation of guest **4** by host $\mathbf{1}^{4+}$ was monitored by measuring the absorbance of the visible charge transfer band that developed upon mixing of the two components. In order to determine the binding constants, a 0.2 mM solution of $\mathbf{1}^{4+}$ in CH_3CN was spectrophotometrically titrated with aliquots from a 50 mM stock solution of the guest **4** which also contained 0.2 mM of $\mathbf{1}^{4+}$ in order to keep the concentration of the receptor constant during the titration. Aliquot addition was continued until a 50-fold excess of the guest **4** was achieved. Corrections for the guest and receptor absorbances at the wavelength of the charge transfer absorption were made. The binding constants were obtained by computer fitting of the experimental absorbance values to the following equations:[7]

$$\frac{\Delta A}{b} = \frac{L_t K \Delta\epsilon [G]}{1+K[G]} \qquad (1)$$

$$G_t = \frac{[G] + L_t K [G]}{1+K[G]} \qquad (2)$$

where ΔA is the absorbance of the charge transfer complex measured at a receptor concentration L_t and a guest concentration G_t, where [G] is the concentration of the guest that is uncomplexed, b is the optical length, $\Delta\epsilon$ is the molar absorptivity of the charge transfer complex, and K is the equilibrium constant for the formation of the complex. The experimental data points were consistent with 1:1 stiochiometry for all complexes. The reported binding constant value was calculated as the average of three independent determinations.

Electrochemical Experiments. The cyclic voltammetry experiments were performed under a purified nitrogen atmosphere. Nitrogen gas was also used to purge all solutions prior to experimentation. Routinely, a constant concentration of 1×10^{-3} M of electroactive species was used. 0.1 M $TBAPF_6$ was added as the supporting electrolyte. Measurements were performed with a small volume (<1 mL), single compartment cell obtained from Cypress Systems (Lawrence, KS). A disk glassy carbon electrode ($0.0079\ cm^2$) and a platinum wire were used as working and counter electrodes, respectively. A small amount of activated neutral alumina was added to the test solution in order to dry *in situ* the solvent/supporting electrolyte system. All potentials were recorded against a Ag/AgCl reference electrode. Half-wave potentials ($E_{1/2}$) were determined as the average of the corresponding anodic and cathodic peak potentials. Standard rate constants ($k°$) for some of the heterogeneous electron transfer processes were determined using the Nicholson procedure[8] from the difference between the anodic and cathodic peak potentials (ΔE_p) observed in cyclic voltammetric experiments.

Results and Discussion

Synthesis. The formation of an inclusion complex between **2** and $\mathbf{1}^{4+}$ was first reported by Harriman and co-workers.[9] Complex formation is quickly demonstrated by the development of an intense blue color upon mixing of **2** and $\mathbf{1}^{4+}$ in CH_3CN solution. As is the case with many complexes of this receptor, color development results from the charge transfer interactions between the aromatic subunits of the electron-deficient host and the electron-rich guest. The binding constant reported for the $\mathbf{2}\cdot\mathbf{1}^{4+}$ complex[9] in acetonitrile ($112\ M^{-1}$) is substantially higher than the corresponding value for 1,4-dimethoxybenzene[1] ($18\ M^{-1}$) which clearly indicated the possibility of using the formation of the $\mathbf{2}\cdot\mathbf{1}^{4+}$ inclusion complex as the core interaction for the template-directed synthesis of a [2]-rotaxane. Therefore, we proceeded to derivatize **2** by

---

(6) Bernardo, A. R.; Stoddart, J. F.; Kaifer, A. E. *J. Am. Chem. Soc.* **1992**, *114*, 10624.

(7) Connors, K. A. *Binding Constants*; Wiley: New York, 1987; Chapter 4.

(8) Nicholson, R. S. *Anal. Chem.* **1965**, *37*, 1351.

(9) Benniston, A. C.; Harriman, A.; Philp, D.; Stoddart, J. F. *J. Am. Chem. Soc.* **1993**, *115*, 5298.

Table 1. Thermodynamic and Spectroscopic[a] Properties of the Inclusion Complexes Formed between Host 1^{4+} and Several π-Donor Guests in CH_3CN at 25 °C

guest	K (M^{-1})	$\Delta G°$ (kcal/mol)	λ_{max} (nm)	ϵ (M^{-1} cm^{-1})
2[b]	112	−2.8	655	712
4	1150	−4.2	672	598
3[c]	1044	−4.1	644	560
6	1100	−4.1	690	700

[a] The spectroscopic properties given correspond to the charge transfer band observed in the visible region. [b] Values for guest **2** taken from ref 9. [c] Values for guest **3** taken from ref 2.

Scheme 1. Synthesis of Rotaxanes 5^{4+} and 7^{4+}

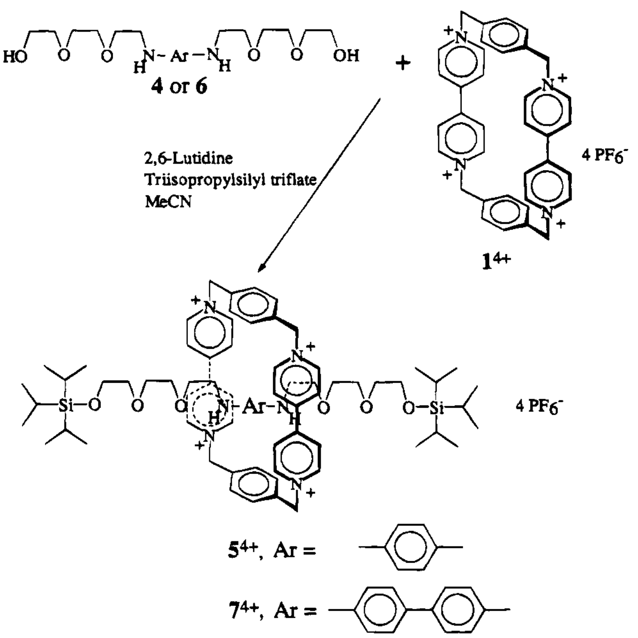

attaching tris(ethyleneoxy) sidearms to both nitrogens, yielding the elongated derivative **4**. Compound **4** was prepared by reaction of **2** with 2-[2-(2-chloroethoxy)-ethoxy]ethanol in K_2CO_3/CH_3CN and purified by column chromatography (25% isolated yield). This compound is extremely susceptible to oxidative degradation as a result of the additional electron density injected by the sidearms into the aromatic nucleus and must be carefully protected from air and light.

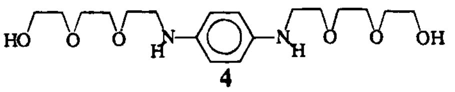

4

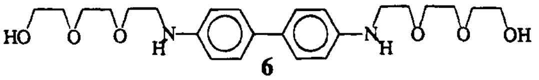

6

The stability constant for the **4**·1^{4+} complex was determined in CH_3CN using the corresponding charge transfer band (λ_{max} = 672 nm). The value obtained is given in Table 1 along with those of other related complexes for comparison purposes. The addition of the ethyleneoxy sidearms to guest **2** increases substantially the stability of its complex with host 1^{4+}. Stoddart and co-workers have shown that the ethyleneoxy sidearms increase the thermodynamic stability of 1^{4+} complexes with guests based on the 1,4-hydroquinol nucleus.[1] The extra stabilization is due to the ion−dipole interactions between the receptor's positively charged nitrogens and the oxygens in the sidearms. The presence of these interactions in the complex between 1^{4+} and **4** is evident from our data. By contrast, these interactions do not seem to play a significant role when the guest's π-donor nucleus is based on the benzidine subunit, as revealed by the similar K values exhibited by the complexes with benzidine (**3**) and its elongated analog (**6**). This is probably due to the longer N−N distance of the benzidine nucleus (as compared to that in 1,4-phenylenediamine) which increases the separation of the ethyleneoxy sidearms from the positive charges of the receptor, substantially weakening the ion−dipole interactions.

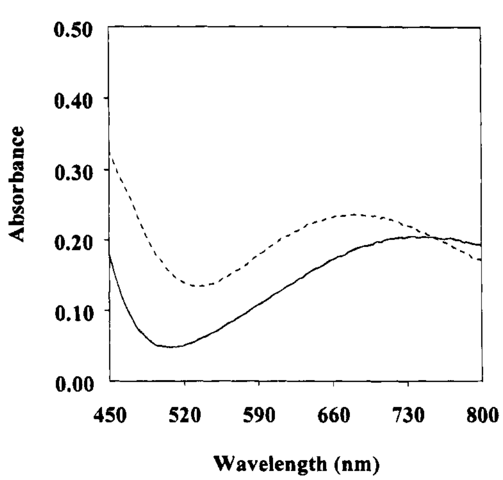

Figure 1. Visible absorption spectra of the rotaxanes 5^{4+} (solid line) and 7^{4+} (dotted line) in CH_3CN at 25 °C. Rotaxane concentration = 0.5 mM. Optical pathlength = 1.0 cm.

Receptor 1^{4+} can be readily trapped in its inclusion complex with **4** by reacting the guest's terminal hydroxyl groups with triisopropylsilyl triflate. This reaction results in the attachment of two bulky triisopropylsilyl stopper groups, yielding the desired turquoise blue, redox-active rotaxane (see Scheme 1). The reaction is quite efficient as judged from the isolated yield of the rotaxane (43% calculated from the amount of receptor 1^{4+} used). This yield is high compared to typical values for related rotaxane formation reactions in which host 1^{4+} is used as the bead.[1] The thermodynamically stability of the complex between **4** and 1^{4+} is the primary factor responsible for the high yield of rotaxane 5^{4+}. We note that similarly high yields of rotaxane are obtained using partially decomposed **4** (about 90% impure by ^1H NMR) as the starting material. The template-directed character of the reaction requires that the generation of the rotaxane be preceded by the formation of the inclusion complex. Thus, the presence of degradation products from **4** does not adversely affect the formation of the rotaxane as the host selectively binds to derivative **4**, while rejecting its degradation products.

The visible spectrum of rotaxane 5^{4+} (see Figure 1) shows a charge transfer band at 745 nm (ϵ = 420 M^{-1} cm^{-1}). This wavelength is longer than those observed for the charge transfer bands of the **2**·1^{4+} and **4**·1^{4+} complex. Similarly, the benzidine-based rotaxane 7^{4+} exhibits a λ_{max} value of 683 nm (ϵ = 480 M^{-1} cm^{-1}), which is longer than that found in the complex with **3**, and slightly shorter than that of the **6**·1^{4+} complex (see Table 1). These observations are generally consistent with the expected red shift of the charge transfer band as the interaction between the π-donor station and the host is facilitated by the molecular architecture. Furthermore, the charge transfer band of 5^{4+} exhibits a longer λ_{max} value than that of 7^{4+} reflecting the fact that the

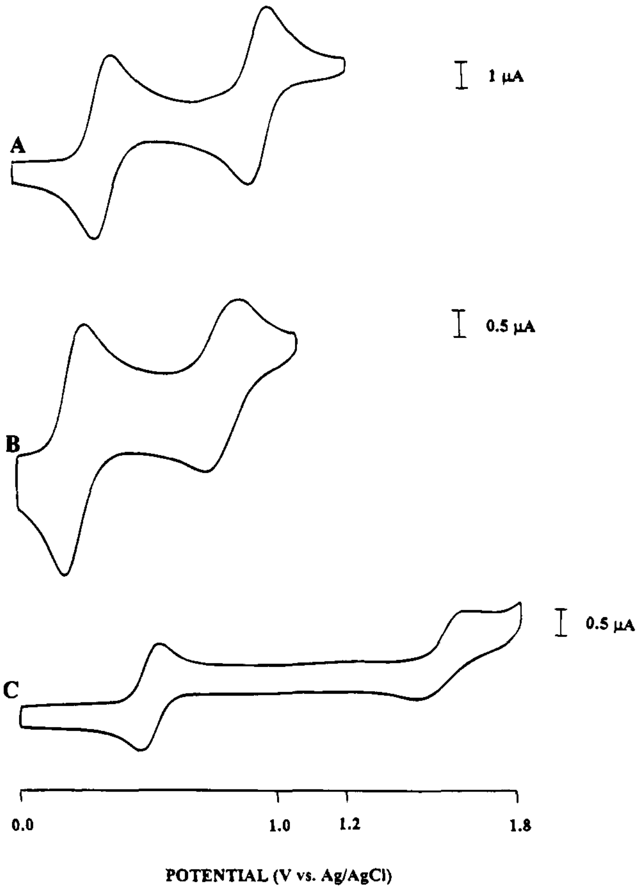

Figure 2. Anodic voltammetric response in CH_3CN/0.1 M $TBAPF_6$ at 25 °C of (A) 1.0 mM **2**, (B) 1.0 mM **4**, and (C) 1.0 mM **5**$^{4+}$. Working electrode: glassy carbon (0.0079 cm^2). Scan rate = 0.2 V/s. Anodic currents plotted upward.

oxidation potential of 1,4-phenylenediamine is lower than that of benzidine (vide infra).

Electrochemistry. Rotaxane **5**$^{4+}$ exhibits a rich electrochemistry due to the redox-active character of the 1,4-phenylenediamine residue[10] in the thread and the 4,4′-bipyridinium[11] (paraquat or viologen) groups in the macrocyclic bead. In order to better analyze the anodic electrochemical behavior of rotaxane **5**$^{4+}$ it is necessary to survey the behavior of compounds **2** and **4** under similar conditions. The anodic voltammetric behavior of compound **2** is characterized by two consecutive monoelectronic oxidations, according to the following equations:

$$\mathbf{2} - e^- \rightleftharpoons \mathbf{2}^{\bullet+} \qquad (3)$$

$$\mathbf{2}^{\bullet+} - e^- \rightleftharpoons \mathbf{2}^{2+} \qquad (4)$$

Table 2. Anodic Voltammetric Parameters of Several 1,4-Phenylenediamine and Benzidine Derivatives in CH_3CN/0.1 M $TBAPF_6$ at 25 °C

compound	D_0 (cm^2/s)	$E^1_{1/2}$ (V)	$k^{o,1}$ (cm/s)	$E^2_{1/2}$ (V)	$k^{o,2}$ (cm/s)
2	1.6×10^{-5}	0.324	>0.02	0.871	>0.02
4	5.4×10^{-6}	0.203	>0.02	0.732	0.006
5^{4+}	3.1×10^{-6}	0.463	>0.02	1.505	0.002
3	1.6×10^{-5}	0.591	–	0.800	–
6	2.2×10^{-6}	0.529	>0.02	0.714	>0.02
7^{4+}	1.4×10^{-6}	0.695	0.006	0.998	0.003

In CH_3CN, at 25 °C, both electron transfer (ET) processes are fast enough to yield diffusion controlled behavior. A typical cyclic voltammogram is shown in Figure 2A. The half-wave potentials ($E_{1/2}$) and other relevant voltammetric parameters are given in Table 2. The anodic voltammetric behavior of compound **4** is very similar (see Figure 2B). The half-wave potentials for the two consecutive monoelectronic oxidations are more negative than the corresponding values for **2**, i.e., both oxidations are thermodynamically easier as a result of the additional electron density injected by the sidearms into the aromatic nucleus of **4**. The negative shift in the $E_{1/2}$ values is consistent with our observations on the greater tendency of compound **4** to undergo oxidative decomposition reactions. Another difference between the electrochemistry of **4** and **2** is that the second oxidation process becomes noticeably slower for the elongated derivative. In fact, the **4**$^{2+}$/**4**$^{\bullet+}$ redox couple can no longer be considered reversible at the scan rates of our experiments (50−500 mV/s).

In compound **5**$^{4+}$ the 1,4-phenylenediamine nucleus is forced by the molecular architecture of the rotaxane to remain inside or in the vicinity of the tetracationic bead's cavity. This molecular configuration exerts a pronounced effect on the anodic electrochemical parameters due to the imposed proximity of the phenylenediamine subunit to the tetracationic macrocycle. First, the half-wave potentials of the two monoelectronic oxidations are substantially shifted to more positive values (see Figure 2C). Both oxidation processes are hindered by the tetracationic macrocycle, which establishes a thermodynamic barrier for the generation of additional positive charges in the system. The situation is pictorially described in Scheme 2. Compared to **4**, the half-wave potential for the first oxidation is anodically shifted by 260 mV (this shift can be partially attributed to the charge transfer stabilization of the 1,4-phenylenediamine subunit when included in the macrocyclic bead's cavity). More surprisingly, the $E_{1/2}$ value of the second oxidation process is shifted by a remarkable 773 mV. In addition to this extraordinary thermodynamic effect, the second oxidation process exhibits even slower ET kinetics than in compound **4**.

It is illustrative to compare these electrochemical results with those obtained with compounds, **3**, **6**, and **7**$^{4+}$. These three compounds can be formally derived from **2**, **4**, and **5**$^{4+}$, respectively, by exchange of the 1,4-phenylenediamine for benzidine subunits. Compound **3** exhibits two consecutive monoelectronic oxidations (see Figure 3A). The potential differences between the anodic and cathodic peaks are substantially smaller than 57 mV in both redox couples, suggesting the possibility of benzidine adsorption to the electrode surface. The elongated benzidine derivative (compound **6**), however, exhibits perfectly reversible voltammetric behavior for both redox couples. As was the case with the 1,4-phenylenediamine substrates, sidearm attachment results in substantial shifts of both $E_{1/2}$ values to less positive values (see Figure 3B). In the corresponding rotaxane (compound **7**$^{4+}$), the presence of the positively charged macrocyclic bead shifts both half-wave potentials to values considerably more positive than those of compound **6** (Figure 3C). The corresponding anodic potential shifts are 166 and 284 mV, for the first and second oxidation processes, respectively. As in **5**$^{4+}$, the four positive charges of the bead destabilize the oxidized

---

[10] Kapturkiewicz, A.; Jaenicke, W. *J. Chem. Soc. Faraday Trans. 1* **1987**, *83*, 2727.

[11] Bird, C. L.; Kuhn, A. T. *Chem. Soc. Rev.* **1981**, *10*, 49.

Scheme 2. The Effects of Core Oxidation in a Rotaxane and Its Parent Inclusion Complex

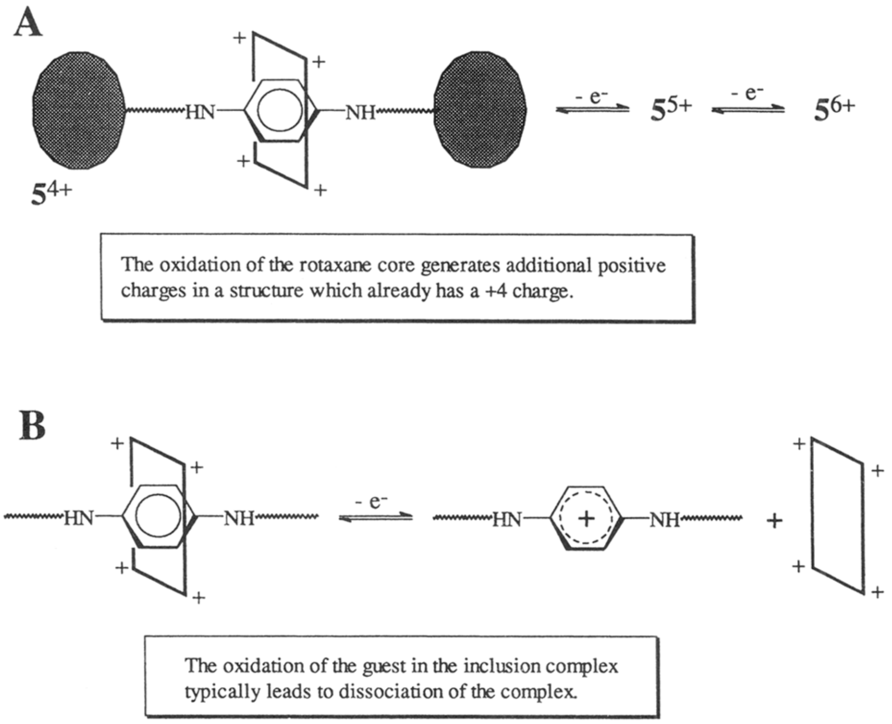

The oxidation of the rotaxane core generates additional positive charges in a structure which already has a +4 charge.

The oxidation of the guest in the inclusion complex typically leads to dissociation of the complex.

forms of the benzidine redox couples, thermodynamically hindering the generation of additional positive charges in the rotaxane. However, this thermodynamic effect is less pronounced in $\mathbf{7}^{4+}$ than in $\mathbf{5}^{4+}$, a difference which is probably the result of the larger size of the benzidine subunit—as compared to 1,4-phenylenediamine—and the concomitant positive charge delocalization over substantially larger Π molecular orbitals. Furthermore, the ET kinetics of the second oxidation process is also slowed down in $\mathbf{7}^{4+}$ by the forced vicinity of the tetracationic bead, but the magnitude of the effect is again smaller than in $\mathbf{5}^{4+}$.

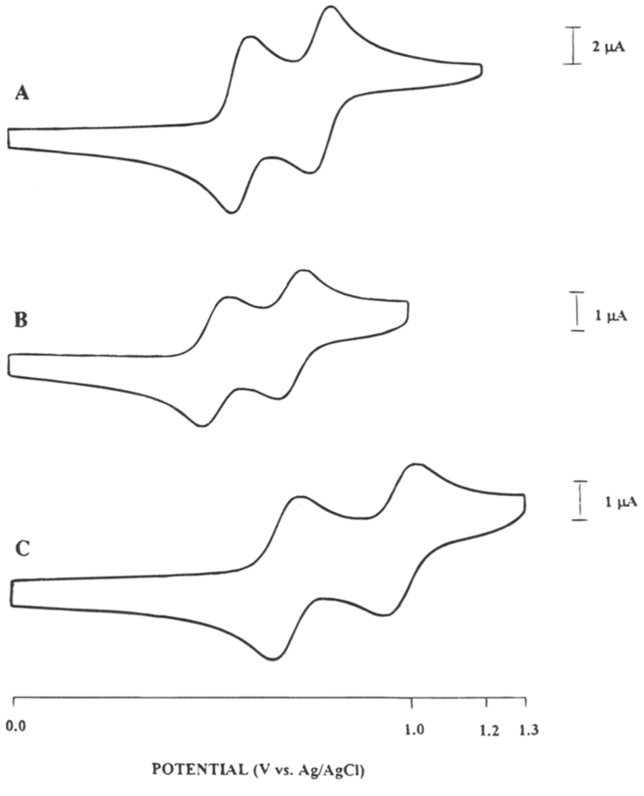

Figure 3. Anodic voltammetric response in CH_3CN/0.1 M $TBAPF_6$ at 25 °C of (A) 1.0 mM **3**, (B) 1.0 mM **6**, and (C) 1.0 mM $\mathbf{7}^{4+}$. Working electrode: glassy carbon (0.0079 cm^2). Scan rate = 0.1 V/s. Anodic currents plotted upward.

The cathodic electrochemistry of the rotaxanes is dominated by the reduction of the two paraquat (PQT^{2+}) groups of the macrocyclic bead. The parent macrocycle (host $\mathbf{1}^{4+}$) undergoes two consecutive two-electron reductions in CH_3CN, with $E_{1/2}$ values of −0.251 and −0.689 V vs Ag/AgCl. The first potential corresponds to the uptake of one electron by each paraquat group ($\mathbf{1}^{4+}/\mathbf{1}^{2+}$ redox couple), while the second potential corresponds to the $\mathbf{1}^{2+}/\mathbf{1}$ couple. The cathodic behavior of this macrocycle as a component of the rotaxanes $\mathbf{5}^{4+}$ and $\mathbf{7}^{4+}$ is shown in Figure 4. The voltammograms show cathodic and anodic scan segments to allow the comparison of the current levels observed in these two potential regions. Clearly, the reduction waves exhibit roughly twice the current levels of the oxidation waves, confirming that the former correspond to two-electron reductions while the latter result from one-electron oxidation processes. The shape of the first two-electron reduction wave of $\mathbf{5}^{4+}$ suggests that the two individual PQT^{2+}/PQT^{+} processes are better resolved than they are in $\mathbf{7}^{4+}$. In order to verify this observation, we surveyed the cathodic behavior of these two compounds using square wave voltammetry (SWV), a more powerful technique for the resolution of voltammetric waves having close $E_{1/2}$ values. The results are given in Figure 5 and show that the $\mathbf{5}^{4+}/\mathbf{5}^{2+}$ process can be resolved into two close redox waves, having half-wave potentials of −0.272 and −0.362 V vs Ag/AgCl. Under the same voltammetric conditions the $\mathbf{7}^{4+}/\mathbf{7}^{2+}$ process cannot be resolved into two waves (see Figure 5). However, we were able to resolve the two monoelectronic waves by using more demanding voltammetric parameters[12] (data not shown). The two half-wave

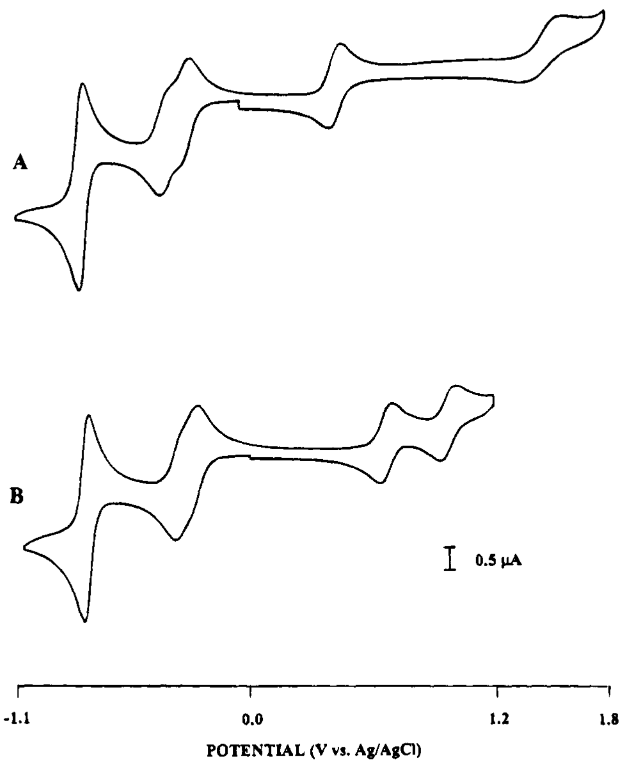

Figure 4. Full voltammetric response of the (A) rotaxane 5^{4+} and (B) rotaxane 7^{4+} in CH_3CN/0.1 M $TBAPF_6$ at 25 °C. Working electrode: glassy carbon (0.0079 cm^2). Scan rate = 0.2 V/s. Anodic currents plotted upward.

potentials are −0.265 and −0.317 V vs Ag/AgCl. The uptakes of the third and fourth electrons take place simultaneously in both rotaxanes. The measured half-wave potential was identical within experimental error for both compounds (−0.780 V vs Ag/AgCl).

We have previously observed in catenane systems[1] incorporating the tetracationic host 1^{4+} that the first reduction process (4+/2+ couple) was resolved into two monoelectronic voltammetric waves. However, the resolution of the two monoelectronic processes involved in the 4+/2+ couple was always the result of different environments for the two paraquat groups, reflecting the distinct molecular architecture of catenanes. Compound 5^{4+} is the first rotaxane (with 1^{4+} as the bead) in which a substantial difference (90 mV) is found between the half-wave potentials of the 4+/3+ and 3+/2+ redox couples. Since environmental differences between the two paraquat groups cannot be invoked in this case, we must conclude that the difference between the two $E_{1/2}$ values is due to a good degree of electronic communication between the two paraquat subunits which is mediated effectively by the 1,4-phenylenediamine subunit.

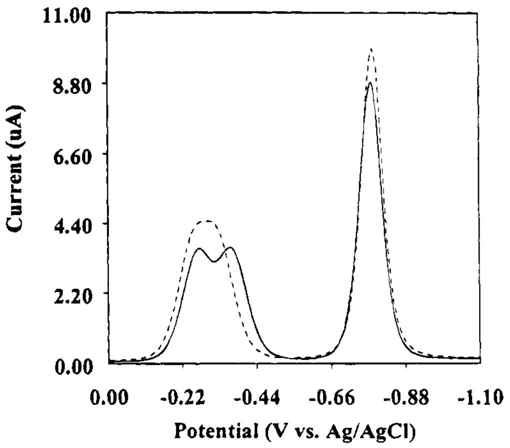

Figure 5. Cathodic SWV response of rotaxane 5^{4+} (solid line) and rotaxane 7^{4+} (discontinuous line) in CH_3CN/0.1 M $TBAPF_6$ at 25 °C. Working electrode: glassy carbon (0.0079 cm^2). Voltammetric conditions: frequency = 15 Hz, square wave amplitude = 25 mV, and potential step = 4 mV.

Conclusions

In summary, we have demonstrated that **2** is an effective guest for complexation by the electron-deficient receptor 1^{4+}. 1,4-Phenylenediamine can be derivatized to template the synthesis of a redox-active rotaxane (5^{4+}). We have shown that, as this synthesis is driven by the formation of a thermodynamically-stable inclusion complex, the [2]rotaxane can be prepared with high yields. Furthermore, the electrochemical behavior of 5^{4+} reveals a remarkable stabilization (increased resistance to oxidation) of the phenylenediamine subunit in the rotaxane. We have already incorporated benzidine as an active π-donor station in the design of controllable (switchable) molecular shuttles.[3] The electrochemical results of this work seem to indicate that 1,4-phenylenediamine is an even more promising subunit regarding its ability to repel the tetracationic bead upon oxidation.

The preparation of complicated molecules, such as rotaxanes and catenanes, in which several cyclic or linear components are mechanically intertwined or locked together is becoming increasingly common. An interesting question arises in these systems regarding the changes in the properties of one of the components that result from its forced spatial relationships to the remaining components. Our findings with rotaxane 5^{4+} demonstrate that some of these effects can be very substantial, altering both the thermodynamic and kinetic behavior of the system.

Acknowledgment. The authors are grateful to Peter Ashton, School of Chemistry, University of Birmingham, for obtaining FAB mass spectra of the two rotaxane samples. A.E.K. thanks the NSF (grant CHE-9304262) for the generous support of this research. E.C. thanks the Department of Education for a Patricia R. Harris Minority Graduate Fellowship.

JO941974A

---

[12] The optimum set of parameters to accomplish the resolution of the two cathodic waves was found to be: frequency, 10 Hz; square wave amplitude, 8 mV; and potential step, 1 mV. The small square wave amplitude and potential step values favor the resolution of waves having close half-wave potentials.